PHYSICAL AND TOPOGRAPHIC FACTORS AFFECTING SUSPENDED PARTICULATE MATTER COMPOSITION IN A SHALLOW TROPICAL ESTUARY

*Yu Umezawa[1], Teruhisa Komatsu[2], Masumi Yamamuro[3] and Isao Koike[4]

1. Faculty of Fisheries, Nagasaki University 1-14 Bunkyo, Nagasaki-city, Nagasaki, 852-8521, Japan

2 Behavior, Ecology and Observation Systems Laboratory, Ocean Research Institute, The University of Tokyo, Minamidai 1-15-1, Nakano, Tokyo 164-8639, Japan

3 Department of Natural Environmental Studies, Institute of Environmental Studies Graduate School of Frontier Sciences, The University of Tokyo, 5-1-5, Kashiwanoha, Kashiwa-shi, Chiba, 277-8562, Japan

4 University of the Ryukyus, Senbaru, Nishihira, Okinawa 903-0123, Japan

*Corresponding author:
E-mail: umezawa@nagasaki-u.ac.jp
Tel: +81-95-851-2849
Fax: +81-95-851-2799

Abstract

To better understand topography-dependent characteristics of suspended particulate matter (SPM) in a tropical shallow estuary during dry season, the physical factors causing an increase of SPM and the sources of SPM were investigated at the western coast of Thailand. Single and multiple regression analyses using physical parameters as independent variables indicated that periodic tidal current-driven resuspension, episodic wind-driven resuspension, and river-borne inputs were the most important factors controlling SPM increases in areas surrounded by sand bars, areas directly facing the ocean, and areas close to the river mouth , respectively. The assessment of the origin of increased SPM over the background levels estimated from the chemical signatures ($\delta^{13}C$ and C/N ratio) at all investigated location and for each event responsible for an increase in SPM confirmed the results of the multiple regression analyses. The results suggested that specific characteristics of SPM at each location were highly contributed by sedimentary materials and could be rather consistent through the season under similar weather conditions.

Key words: Resuspension, suspended particulate matter (SPM), stable isotopes, mangrove, estuaries, multiple regression analysis, seafloor morphology, Thailand

1. Introduction

The topographic characteristics of shallow estuaries vary in terms of depth and distance from the river mouth, sand bars, and open ocean. Estuaries also contain varying forms of suspended particulate matter (SPM), including autochthonous planktonic matter, land-derived river-transported matter, debris from vegetation (e.g., mangroves and seagrasses), and resuspended sedimentary organic matter (SOM) (Cifuentes et al., 1988, 1996; Bodineau et al., 1998; Dittmar, 2001). The quantity and characteristics of SPM in estuarine waters fluctuate temporally and spatially and influence a number of biological processes, including food availability for bivalves (Bacon et al., 1998; Ellis et al., 2002) and light availability for seagrasses (Longstaff and Dennison, 1999). Therefore, it is important to understand the temporal variability of SPM qualities and quantities in estuaries at a spatial resolution that allows us to account for differences in the composition and physiological characteristics of resident benthos species.

In a river-dominated estuary, the quality and quantity of particulate organic matter (POM) depend mainly on land use within the watershed (Howarth et al., 1991; Correll et al., 2001; Carmichael and Valiela, 2005), and the POM distribution varies with the distance from the river mouth and the amplitude of tidal cycles (Rezende et al., 1990). However, in tropical and subtropical shallow estuaries, much POM, including mangrove-derived debris, becomes trapped in mangrove swamps or settles at the bottom of meandering streams due to salt flocculation, tidal pumping, and biological effects (Gibbs and Konwar, 1986; Wolanski, 1995; Furukawa et al., 1997; Wolanski and Spagnol, 2003). As a result, the transportation range of POM is narrower than that of dissolved organic matter (Dittmar et al., 2001). Furthermore, in mangrove estuaries with undeveloped catchments, resuspension of sediments can be a major autochthonous factor compared to planktonic primary production, because mangrove swamps have the capacity to absorb river-borne nutrients (Trott and Alongi, 2000).

Increased turbidity due to sediment resuspension, particularly from wind-driven disturbances, has frequently been observed in shallow water ecosystems (Luettich et al., 1990; Smaal and Haas, 1997; Oldham and Lavery, 1999; Douglas and Rippey, 2000). Strong tidal currents caused by a large tidal range can also cause sediment resuspension and transport (Alvarez and Jones, 2002; Wolanski and Spagnol, 2003). The contributions of these mechanisms likely differ by location within shallow estuaries having complex geomorphology, although more research is needed to assess the mechanisms causing resuspension and the variability of these mechanisms. While the ratio of particulate organic carbon (POC) to chlorophyll *a* (POC/chl. *a*) has been effectively used as an index of the relative contribution of resuspended sediment to SPM (Cifuentes et al., 1996; Miyajima et al., 1998), it does not allow for identification of the sediment. In contrast, mass balance equations consider the specific chemical

signatures of land-derived POM and several primary producers living in estuaries and along shorelines, allowing researchers to infer the spatial and temporal contributions of these sources to the POM of estuary waters (Dittmar et al., 2001; Goñi et al., 2003; Kennedy et al., 2004). Because SOM characteristics vary widely compared to those of other POM forms within an estuary (Meksumpun and Meksumpun, 2002), an inventory of SOM characteristics according to location and/or substrate could help in identifying the area supplying SOM in the water column.

Our objectives in this study were to (i) examine whether SOM in our target areas actually had location-specific chemical endmembers that could be used for source identification, (ii) identify the physical factors controlling a SPM increase at each location with specific topographic locations, and (iii) evaluate SPM source for increased SPM events based on chemical compositions. We sampled SOM and spatiotemporally monitored the chemical signatures of SPM and physical parameters (i.e., turbidity, wind and current speed and direction, salinity, and water depth) at three adjacent subtidal areas in Thailand. The extent to which each representative factor (i.e., wind- and/or current -derived resuspension, river water inputs) contributed to increasing SPM was evaluated by simple and multiple correlation analyses between turbidity and the above factors. As partly reported in previous studies (Andrews et al., 1998; Dittmar et al., 2001; Gacia et al., 2002; Goñi et al., 2003; Kennedy et al., 2004), the carbon stable isotope ratio ($\delta^{13}C$) and C/N ratio of POM in river and surface sediments collected throughout the estuary could be used to distinguish the sources of organic matter; these sources could be primarily be divided into resuspended sediments and other background sources (river-borne POM and marine-derived POM).

2. Materials and Methods

2.1. *Study site*

The study took place in a shallow estuary located about 130 km north of Phuket on the western coast of Thailand (9° 10'-17' N, 98° 18'-28' E; Fig. 1). The land areas along the coast and lower river stream are populated by dense mangrove forests, with a patchy distribution of small fisheries and villages. The rainy season, having monthly rainfall of over 600 mm on average, occurs from May to October, while the rest of the year constitutes the dry season with less than 100 mm of precipitation (mean data from 1971-2000; Thai Meteorological Department). Recent 5-year wind data show that about 65% of the maximum winds come from the north during the dry season (Thai Meteorological Department). The Khura River (20-25 km in length) and other small rivers and tidal creeks flow into this estuary. Intertidal and sub-tidal areas covered by dense seagrass beds (*Cymodocea rotundata, Enhalus acoroides, Halophila ovalis*, and *Syringodium isoetifolium*) range along the coastline near the sampling sites of Ko Chong, Mai Hang, and Thung Nang Dam being closest to farthest from the river's outlet (hereafter designated as KC, MH and TND; Fig. 1). The tidal oscillation in these areas varied between 1.5 m (neap tide) and 3.5 m (spring tide). The seagrass bed at TND was nearly 75% surrounded by an intertidal sand bar, which rose 0.5-0.8 m above the flat sea bottom and emerged at low tide. Site MH directly faces the open sea, while KC is located in the channel near the river mouth.

2.2. *Monitoring, sampling, and preparation*

2.2.1. *Water sampling and preparation*

To clarify the mechanisms causing SPM increase, especially, resuspension of sediments, monitoring was conducted in the dry season to avoid the severe influence of river discharge in rainy season. Sampling of seawater for chemical analyses was conducted at the center of each subtidal seagrass bed (Fig. 1) during the daytime (07:00-18:00 local time on 9, 11, and 14 December 2001 at TND; 22, 23, and 27 December 2002 at MH; and 25 and 26 December 2002 at KC). Using 2.5-L polycarbonate bottles, a diver approached the station upstream and collected paired seawater samples (0.2 m below the surface and 0.2 m above the bottom) on an hourly basis. POM samples for the analyses of POC/particulate organic nitrogen (PON) contents and $\delta^{13}C$ were prepared by filtering 1-2 L of seawater through a 300-μm mesh sieve and a pre-combusted (450°C, 3 h) glass fiber filter (GF/F: 0.7 μm pore size); Whatman, Middlesex, U.K.), then gently washing the samples with small amounts of distilled water. The matter captured on the filter was referred to for estimating the size of suspended particulate matter (SPM; mg L^{-1}), after drying at 60°C. The filter samples were fumigated with 12N-HCl for 2 days to remove inorganic carbon. A third- or half-portion of the filter was then placed in an acetone-rinsed tin capsule,

after the remaining HCl and humidity had been removed by vacuum desiccation in the presence of NaOH.

For chl *a* analyses, 100 ml of sea water were filtered through a 25-mm GF/F filter, and the filter was placed in a shaded polypropylene tube with 6 ml of N, N-dimethylformamide (DMF) to extract the pigments. All samples were frozen until the analyses.

2.2.2. *Physical parameters*

A pyramid-shaped frame equipped with an electromagnetic current meter (± 1 cm/s accuracy, COMPACT-EM; Alec Electronics Co., Ltd., Kobe, Japan), salinity meter (± 0.02 mS/cm accuracy, COMPACT-CT; Alec Electronics), and infrared back-scattering turbidimeter (±1 ppm accuracy under 50 ppm of turbidity calibrated in kaolin in the laboratory, and within ± 2% when over 50 ppm, MTB-16K; Alec Electronics) was deployed on the seafloor at each monitoring site. The turbidity, salinity, and current sensors were located at 0.2, 0.4, and 0.5 m above the seabed, respectively. Each parameter was monitored at 3- or 6-minute intervals. Wind speed and direction were monitored by an anemometer (Micro Anemo KC-201; Makino Applied Instruments, Inc., Tokyo, Japan) every 10 to 60 minutes on a boat anchored near the monitoring site. Some irregular values recorded by the turbidimeter, due to signal error or drifting matter lodged in the sensor, were omitted from the analyses. Because *in situ* POC concentrations above the seafloor and kaolin-based turbidity (ppm) acquired during monitoring were highly correlated at each area (r = 0.77-0.98, $P < 0.001$, Fig. 2-a), the values calibrated from hourly POC concentrations were substituted for the lost turbidity data. Further, all kaolin-based turbidity data were also calibrated using *in situ* SPM data for later statistical analyses (Fig. 2-b). At TND and MH, different regression lines were employed according to the magnitude of *in situ* SPM.

2.2.3. *Sediment sampling and preparation*

Two replicate sediment samples for POC/PON contents and $\delta^{13}C$ analyses were collected with an acrylic core (50 mm in diameter) at each of 33 locations (Fig. 1) in December 2001. Specifically, each location was categorized as river stream (st. 1-10), seagrass bed (st. 13, 16, 17, 24, 25, and 26), bare sand areas around seagrass beds (st. 14, 27, and 30), intertidal coarse sand area (st. 22, 23, 28, 31, 32, and 33), shallower channel (st. 11, 12, 15, and 21), and deeper channel (st. 20). The top 10 mm of sediment were transferred to a plastic bag and kept frozen during transportation. Samples were dried at 60°C, manually disassociated into fine particle through the plastic bag, and then sieved through a 300-μm mesh to remove plant fragments, shells, and coarse sand. After powdering with a mill, samples for POC and PON contents were weighed into precombusted (950°C for 1 h) ceramic boats and acidified by the HCl vapor

method to remove inorganic carbon. Samples for $\delta^{13}C$ analysis were acidified by the wash-out method, adding a high-purity 1N-HCl solution until carbon dioxide release was no longer visible. After centrifugation at 1200 *g* for 20 min, the supernatant was discarded, and the sample was rinsed with high purity Milli-Q water to remove any remaining salt components. Despite large loss of organic C by the wash-out method, few alterations of $\delta^{13}C$ have been observed for various types of sediment samples (Midwood and Boutton 1998; Schubert and Nielsen 2000; Umezawa et al 2008). Dried aliquots with sufficient C contents for the analysis were weighed in acetone-rinsed tin capsules.

2.3. *Analytical methods*

Concentrations of chl *a* extracted into DMF were determined fluorometrically (10-AU, Turner Designs, Sunnyvale, CA, USA), and the concentrations in the seawater were calculated (Suzuki and Ishimaru, 1990).

The C and N contents (%) of the processed sediment samples were determined with a CHN analyzer (MT-5, Yanaco, Kyoto, Japan), following the method of Yamamuro and Kayanne (1995). The difference in C and N contents between two (or more) replicate samples was less than 0.04 wt% for C and 0.002 wt% for N, a precision sufficient for the purposes of this study.

The C and N contents and $\delta^{13}C$ of the samples on the filters and of sediment samples were measured using an elemental analyzer (EA1108 or Flash EA, Fisons Instruments, Beverly, MA, USA) and isotope-ratio mass spectrometer (Mat 252 or Delta plusXP, Finnigan, Waltham, MA, USA). The ratio of ^{13}C:^{12}C was calculated as: $\delta^{13}C = \{[R\ (sample) / R\ (standard)]-1\} \times 1000$ (‰), relative to PeeDee Belemnite (PDB), where $R = {}^{13}C/{}^{12}C$. The instrumental precision through $\delta^{13}C$ analyses was 0.24‰ (standard deviation: $n = 40$) and 0.10‰ ($n = 21$) for sediments and filter samples, respectively. Each set of paired core samples was measured twice (i.e., two samples × two replicate measurements), with a mean absolute difference of 0.51‰ for sediment samples and of 0.29‰ for on-filter POM samples.

2.4. *Statistical analyses*

Statistical analyses were carried out using the software packages SPSS 11.0 (SPSS Inc., Chicago, USA) and Statcel ver. 2 (OMS-Publishing, Saitama, Japan). At each study site, the relationships between SPM and three physical parameters to which a rise in SPM was likely attributable (i.e., wind speed, current speed, and river discharge as reflected by salinity) were evaluated by Spearman's rank correlation coefficient. For the relationship with SPM, water depth, which often correlates with current speed and salinity change, was also evaluated to check the tidal conditions under which rises in SPM tended to occur. In areas where more than two concurrent physical factors were significantly correlated to SPM

increase, multiple regression analyses (MRA) were subsequently performed to compare the contribution of each factor to the SPM increase by applying SPM as the dependent variable and other selected physical factors as independent variables. The extent to which each representative factor contributed to an increase in SPM was evaluated by standardized partial regression coefficients. In advance of these analyses, Spearman's rank correlation coefficients between applied physical parameters were calculated to test for multicollinearity among the independent factors. In cases where the SPM data did not have normal distributions, the data were log transformed prior to the analysis. Finally, the contribution of each parameter to SPM increase was considered, based on the standardized partial regression coefficient of each parameter.

2.5. *Estimation of chemical components in additional POM*

The concurrent change in total amounts of SPM and its characteristics could be caused by the influx of other SPM (e.g., newly resuspended SOM and river-derived POM) with specific chemical characteristics into the original background SPM (mainly marine-derived POM) (Sanford, 1994). When the quantity of additional POM is lesser than background POM, identification of its source from chemical signatures in bulk POM can be masked by the values in the original POM. Assuming that shifts in the C/N ratio and $\delta^{13}C$ values in the POM result from the mixture of original background POM with additional POM, therefore, the following simple mass balance equations with two end-members were tentatively applied to better elucidate the source of additional POM. The plausibility of this approach was carefully verified in result and discussion sections, based on the consistency between chemical signatures in estimated source of additional POM and physical agents responsible for the SPM increase.

$$[(POC_{ob} - POC_{bg}) / 12.011] / [(PON_{ob} - PON_{bg}) / 14.0067] = CN_{add} \quad (1)$$

$$POC_{ob} \times \delta^{13}C_{ob} = (POC_{bg} \times \delta^{13}C_{bg}) + (POC_{add} \times \delta^{13}C_{add}) \quad (2)$$

where

POC_{bg}, PON_{bg}, and $\delta^{13}C_{bg}$ are the mean **b**ack**g**round POC (mg L^{-1}), PON (mg L^{-1}), and the $\delta^{13}C$ values (‰) under calm weather conditions, where POC and other chemical parameters were flat with low values (see 3.3);

POC_{add}, CN_{add}, and $\delta^{13}C_{add}$ are POC (mg L^{-1}), C/N molar ratio, and $\delta^{13}C$ values in **add**itional fraction;

POC_{ob}, PON_{ob}, and $\delta^{13}C_{ob}$ are the POC (mg L^{-1}), PON (mg L^{-1}), and $\delta^{13}C$ values of the hourly sampled (**ob**served) seawater;

12.011 and 14.0067 are the elemental masses of carbon and nitrogen, respectively.

3. Results and Discussion

3.1. *Chemical characteristics of sediment organic matter in the estuary*

The chemical composition of SOM from the lower reaches of the river to the estuary showed large variations in C/N ratios (8.0 to 24.1; Fig. 3a), $\delta^{13}C$ (-29.0 to -21.0‰; Fig. 3b), and total organic carbon (TOC) content (0.06 to 4.8%; Fig. 3c). Organic matter accumulated where physical conditions were attenuated by river meanders, deeper water and seagrass leaves (Fig. 3c). The sediment with lower TOC contents showed lower C/N ratios ($r_s = 0.84$, $p < 0.001$; Spearman's correlation). This result may be partially explained as follows. Mobile coarse sand exposed under strong current flows in the TND area could have easily released organic debris into the water column, while exposure to air at low tide for several hours could have stimulated net production of microphytobenthic communities (Blanchard et al., 2001), resulting in relatively low TOC contents (generally < 0.1 %) and lower C/N ratios (< 10.0). On the other hand, the normally distributed C/N ratios and $\delta^{13}C$ values of SOM were significantly correlated ($r = -0.57$, $p < 0.001$; Pearson's correlation; Fig. 4).

In the seagrass beds, materials entrapped by the seagrass leaves and direct supplies of seagrass debris (Gacia et al., 2002; Kennedy et al., 2004) and their decomposition products are generally the main sources for sedimentary organic matter. The $\delta^{13}C$ values of seagrass leaves, roots, and rhizomes (-7.4 to -9.4‰; Yamamuro et al., 2004) and of epiphytes on seagrass leaves (-19.5 ± 1.0‰; Y. Umezawa, unpublished data) collected around this estuary were significantly heavier than those for sediment in seagrass beds (-25.2 ± 0.6‰) (Fig. 4). Even their main refractory component, lignin, which is a ^{13}C-depleted component among tissues by several parts per thousands (Schweizer et al., 1999), was insufficient to explain this large difference; therefore, terrestrial- and mangrove-derived materials trapped by seagrass leaves were likely essential components forming the organic materials in these seagrass beds. The $\delta^{13}C$ values and the C/N ratios in seagrass beds in this estuary were similar to those observed at seagrass beds adjacent to extensive mangrove stands in Southeast Asia (Kennnedy et al., 2004).

Sediments originating in the mid-basin had lighter $\delta^{13}C$ values (-29.0 ± 0.1‰; Fig. 4), suggesting that they were most influenced by organic matter of terrestrial origin, since POM in the upper and middle reaches of streams showed lower C/N ratios and lighter $\delta^{13}C$ values (9.5 ± 1.3 for C/N ratio and -28.4 ± 2.4‰ for $\delta^{13}C$, $n = 7$; M. Minagawa, pers. com.). On the other hand, higher C/N ratios and lighter $\delta^{13}C$ in sediments from lower stream reaches (Fig. 4) would suggest a higher contribution of riverine and coastline mangroves, which have higher C/N ratios and lighter $\delta^{13}C$ (20.0 to 50.0 for C/N, -25.0 to -30.0‰ for $\delta^{13}C$; Kuramoto and Minagawa, 2001). The contribution of land-derived POM with a lower

C/N ratio and the alteration of chemical characteristics by bacterial N immobilization (Benner et al., 1990) might have lowered the C/N ratio from the values found in mangroves leaves.

If resuspended SOM represents a substantial contribution to POM in the water column within the estuary, spatially specific distributions of $\delta^{13}C$ and C/N ratios in SOM (Fig. 4) could potentially be an effective indicator of the POM source. In addition, because the TOC content in sediments also varied at each location, identifying the source area of SOM would be useful for predicting the usual quality of SPM at each area.

3.2. *Mechanisms underlying modulation of turbidity*

The correlation of SPM time series with other physical factors varied noticeably among the study sites: SPM increased at lower tides at MH and KC, but at higher tides at TND (Figs. 5, 6, and 7-a, respectively). Furthermore, significant relationships with SPM increase were confirmed both for current and wind speed at TND, for the wind speed at MH, and for salinity at KC (Table 1). At TND and MH, where multiple physical parameters were correlated with SPM increase to some extent, multiple regression analysis (MRA) was carried out using these parameters (Table 2).

At the TND area, which is surrounded by a large sand bar, standardized partial regression coefficients for current speed and wind speed were 0.63 ($p < 0.001$) and 0.26 ($p < 0.001$), respectively (Table 2). This result clearly suggested that an exponential increase in SPM occurred during high tide, caused primarily by an increase in current speed and synergistically by enhanced wind speed. Salinity was statistically evaluated to be minor factor, probably because salinity was constant throughout the monitoring hours (Fig. 5c). When the current is opposite the wind direction, wave height generally increases, enlarging the shear stress on the bottom (Wolanski and Spagnol, 2003). Although we also observed this effect at our study area (see periods *III*, *IV*, and *V* in Fig. 5-a and b), the magnification of turbidity was not as significant compared to that under other conditions in which stronger currents flowed in the same direction as the wind (periods *I* and *II* in Fig. 5-b). We assumed that sand bars, which emerge at low tide, would protect the shallow subtidal beds from swell-induced turbulence, but that these beds would conversely be vulnerable when exposed to stronger currents at high tide, especially under higher wind conditions.

At MH, on the other hand, the standardized partial regression coefficients were 0.50 ($p < 0.001$) for wind speed and -0.18 ($p < 0.001$) for salinity (Table 2). Wolanski and Spagnol (2003) observed that the threshold current velocity at which erosion began was 0.4 m s^{-1} at intertidal areas of King Sound in northern Australia. The observed maximum current velocities at MH were less than this threshold value (i.e., 0.35 or 0.40 m s^{-1}), suggesting that even the maximum current speeds at MH (periods *I* and *II* in Fig.

6a, b) did not cause substantial resuspension at this sandy flat (at MH, the silt clay content was only 5 to 10%; Tanaka and Nakaoka, 2006). The negative correlation between depth and SPM (Table 1) indicated that the SPM in the MH subtidal area, which faces offshore without any barrier, was greater at low tide (periods *III* and *IV* in Fig. 6a). Under critical water levels, swell and wind-derived shear stress probably easily detached bottom materials. Because the water-depth threshold disturbed by wind-induced waves is generally defined by a combination of wind speed and fetch length (Douglas and Rippey, 2000), further increases in SPM may be expected under greater wind speeds, even at high tide. However, the effects of biological factors such as biofilm and bioturbation on resuspension should also be considered when examining the threshold of physical factors causing resuspension (e.g., Widdows et al., 2000).

At KC, the SPM source could be the brackish water originating in the upper reaches of streams rather than seawater flowing back from the lower reaches of streams because high turbidity was observed more often during the later lowest tide than during the ebb tide (periods *I* and *II* in Fig. 7a). An alternative explanation is that autochthonous plankton increased in this water body as it constantly flowed in and out of the river mouth and lower streams. This hypothesis was supported by the lower POC/chl *a* ratio accompanied by the POC increase during low tide at KC (see below). These results and the location of the KC subtidal bed near the river mouth correspond with the results of the statistical analysis, which showed a significant inverse linear correlation between SPM and salinity (Table 1).

Regression analyses of SPM concentrations with physical parameters clearly indicated that changes in SPM concentrations in subtidal areas were explained by different combinations of physical agents according to the seafloor topography.

3.3. *Characterization of SPM and validation of defined background values*

It was assumed that the effect of resuspension on SPM can be emphasized at bottom areas, which could enable us to easily identify the SPM sources using chemical signatures at bottom layer. However, despite the variation of water depths (about 0.4 to 2.6 m at TND and MH, and 1.4 to 3.8 m at KH), most chemical signatures of SPM collected near the bottom showed trends similar to those collected near the surface, excluding the period when higher SPM concentrations were observed at TND during high tide (data not shown). Therefore, the discussions below are based on the surface SPM data (Figs. 5, 6, and 7).

Across the monitoring period at both TND and MH, POC contents were significantly correlated (Spearman's) with the $\delta^{13}C$ value (r_s = -0.78 and -0.75, $P < 0.001$, respectively; Figs. 5 and 6-e, f), C/N ratio (r_s = 0.97, 0.78, $p < 0.001$, respectively; Figs. 5 and 6-e,f), and chl. *a* contents (r_s = 0.80 and 0.61, $p < 0.05$, respectively; Figs. 5 and 6-e, g), whereas these relationships were not significant at KC (Figs. 7-e, f, g). A possible explanation is that the greater POC at TND and MH were always drawn from POC of

similar sources, whereas POC from various sources contributed to the increase of POC at KD.

When POC values and other chemical parameters were flat with low values (e.g., mostly less than 0.2 mg L^{-1} for POC), the C/N ratios (8.3 ± 0.6; Figs. 5, 6, and 7-f) at all sites under these calm conditions fell within the range of typical values for living phytoplankton (i.e., 6 to 10, Cifuentes et al., 1988). These C/N ratios shifted up to 12.0 at TND, 12.1 at MH, and 9.7 at KC under higher POC conditions, with occasional decrease to as low as 7.1 at KC. Furthermore, the lower POC/chl *a* during these periods at each site (209 ± 35, 249 ± 59, and 187 ± 29 for TND, MH, and KC, respectively; Figs. 5, 6, and 7-d) also support the substantial contribution of phytoplankton to POC composition (cf., Cifuentes et al., 1988). Slightly higher (>200) POC/chl.*a* levels, especially at MH, and the concurrent lower POC/SPM values (2.0–6.0 wt. %; Fig. 6d) suggested that these SPM under calm conditions still included remaining sedimentary detritus, probably resuspended during prior events. However, this planktonic organic matter with less sedimentary detritus was considered appropriate as the typical background value for later analyses (section 3.4). The $\delta^{13}C$ values of background SPM, which increased with the distance from the river mouth (i.e., from -24.2 ‰ at KC to -22.4 at TND; Appendix 1) might partially reflect the $\delta^{13}C$ difference in the source dissolved inorganic carbon (DIC) for autochthonous phytoplankton, as reported for seagrass leaves in mangrove estuaries (Hemminga et al., 1994). Similar to the variation of C/N and POC/chl *a* values, the $\delta^{13}C$ values (-23.5 ± 0.8‰) were fairly constant throughout the estuary under lower POC conditions, but shifted up to -24.5‰ at TND, -25.5‰ at MH, and -28.0‰ at KC with the mixture of other additional POC (Figs. 5, 6, and 7-f).

3.4. *Model validation and identification of the additional SPM sources*

The following two type of evidences from time-series data indicate that resuspended sediments were likely the main source of increased SPM, especially at TND and MH: (i) increased turbidity was strongly correlated with an increase in current speed and wind speed (see 3.2), and (ii) as POC increased, POC/chl.a shifted farther from the typical values of planktonic POM (see 3.3). Furthermore, the different shifts of $\delta^{13}C$ and C/N values in SPM and different slope values associated with the POC and turbidity relationship (Fig. 2a) suggested that the sources of additional SPM varied among the locations. Because the $\delta^{13}C$ and C/N ratio in sediments within estuaries showed fine-scale variations (Fig. 4), such chemical signatures in SOM could be applied to identify the sources of additional SPM.

Since the chemical characteristics of background SPM were rather constant (3.3), and high SPM events could be made up of background SPM and additional SPM, we could estimate the chemical characteristics of the additional SPM ($\delta^{13}C_{add}$ and CN_{add}) by subtracting the chemical signatures of background SPM ($\delta^{13}C_{bg}$ and CN_{bg}) according to equations 1) and 2) (see 2.5). Most $\delta^{13}C_{add}$ and CN_{add}

showed clear variations by location (Appendix 1), with their distribution seemingly depending on the tidal condition and wind condition, regardless of the monitoring day (Fig. 8). To validate this new approach, we verified whether the sources suggested by chemical components were actually supported by the physical and topographical factors causing an increase of SPM.

At TND, the estimated values for the additional SPM at lower tide overlapped with the range for bare sand areas around the seagrass beds (Fig. 8). Under conditions in which weak wind-induced waves were only strong enough to disturb sediments in bare sand areas (st. 27 and 29) (3.2), attenuation of the physical disturbance within the seagrass beds (cf. Madsen et al., 2001; Peterson et al., 2004) would have prevented sediment resuspension in the seagrass meadows (st. 24, 25, and 26). In contrast, sediments in both the seagrass beds (st. 24 and 26) and the intertidal coarse sand area (st. 31 and 32), which could be vulnerable to stronger currents and wind-induced waves (3.2), would have been main sources of SPM during higher tide. These suggestions correspond to the finding that $\delta^{13}C_{add}$ and CN_{add} values during higher tide were between the values for seagrass beds and coarse-sand areas (Fig. 8).

At MH, which faces the outer ocean and where resuspension by wind-induced disturbance and river-derived matter were concluded to be the main mechanisms causing turbidity (3.2), the additional SPM had four to five times higher C/N ratios under higher wind conditions than under lower wind conditions (Fig. 8). This was probably caused by dominant northerly wind-induced swells and waves along a lengthy fetch; these swells would have created enough shear stress to disturb sediments in shallower channels (st. 21) and even in seagrass beds (st.16), which had higher C/N ratios. On the other hand, $\delta^{13}C_{add}$ and CN_{add} values clearly differed between ebb tide and low slack tide by 2‰ for $\delta^{13}C$ and by a factor of 4 for the C/N ratio, regardless of wind conditions (Fig. 8). As suggested by statistical analyses (3.2) and the POC/chl.*a* value of approximately 200 at low tide, some POM contributions may have been of riverine origin with low C/N.

At KC, the $\delta^{13}C_{add}$ and CN_{add} values also differed according to tidal conditions. The source of additional SPM at lowest tide was considered to be mainly terrestrial POM because the $\delta^{13}C$ values fell in the range of POM collected in the upper or middle reaches of streams (Fig. 8). The lower estimated C/N ratio may suggest POM fluxes from fish ponds (cf., Jackson et al., 2003) and autochthonous phytoplanktonic contributions. This speculation based on the chemical signatures was consistent with statistical analyses showing that river water flow caused turbidity in the water column at KC (see 3.2). On the other hand, heavier $\delta^{13}C$ and slightly higher C/N ratio in additional POM observed during ebb tide, may reflect sedimentary POM, which had similar $\delta^{13}C$ and C/N values in surrounding areas (st. 8 and 12) (Fig.8).

The calculated CN_{add} and $\delta^{13}C_{add}$ provided useful information regarding the sources of additional

SPM at each subtidal seagrass bed, although many potential complex disparities could exist between calculated values and the suggested sources: (i) POM may have undergone selective resuspension and settling during transport (Miyajima et al., 1998); (ii) additional POM may have been delivered simultaneously from a mixture of different sources including epiphytic detritus; (iii) within a given area, sedimentary POM may have had a heterogeneous composition, as suggested by the significant disparities between duplicate sediment samples; and (iv) acid-soluble organic matter lost during the washout-method for sediment samples would account for some of the difference between their C/N values and those of the original bulk values (Yamamuro and Kayanne, 1995).

In this study, however, the origins of increased SPM estimated from the combined chemical signatures at each location agreed well with observed characteristics of physical agents for the events responsible for SPM increase (e.g., direction of lateral advection, wind-derived vertical shear stress, and salinity change). Therefore, the trial approach introduced in this study (i.e., separation of bulk POM into background and additional fractions) seemed to work well in approximately identifying the source area of resuspension when there were relatively small variations in the values for the above-mentioned factors compared to the variation in the values for potential POM sources.

3.5. *Expected responses of benthic organisms to the regular pattern of SPM characteristics*

Given that the sediment characteristics and independent physical factors leading to rises in SPM were variable at each site, it was not surprising that time-averaged SPM characteristics (POC/N ratio and POC/SPM ratio) also differed among the sites within a small estuary. That is, lower POC/SPM and higher C/N ratios of POM were constantly observed at TND (Fig. 5d, f), whereas extraordinarily higher POC/SPM and lower C/N ratios of POM were observed at KC (Fig. 7d, f). Although tidal current-induced resuspension periodically disturbed water quality at TND, the water quality at MH and KC was more closely related to weather conditions, namely wind speed and rainfall, respectively. Therefore, during the dry season when weather conditions are mostly steady, specific characteristics of SPM at each location could be rather consistent.

Different chemical fluxes in the water column affect potential food supplies and light availability for benthic and planktonic organisms. For example, elevated turbidity and nutrient levels reduce the penetration of light for benthic macrophytes (Longstaff and Dennison, 1999; Moore and Wetzel, 2000) and the potential food quality for benthic filter feeders (Small and Hass, 1997; Ellis et al., 2002). Location-specific SPM characteristics may be a key environmental factor explaining the differentiations of biological communities within a few square kilometers in this estuary. For example, cockles growing at KC have longer shell lengths than cockles in other areas (Suzuki, 2003). In addition to such refractory

organic matter, the contribution of marine phytoplankton-derived labile organic matter, which has shorter residence time in the water column, should also be further examined (Zimmerman and Canuel, 2001).

The topography of a tidal flat is easily changed by long-term gradual accretion and short-term episodic erosion associated with strong tidal currents, wave action, and wind forcing (Mazda et al., 1990; Dyer et al., 2000; Uchiyama, 2001). These morphological alterations would significantly affect benthic ecosystems not only by the direct effects of sedimentation (Preen et al., 1995), but also by altering the quantity and quality of SPM supplied in the overlying water column.

4. *Conclusions*

Microalgae-mediated coupling between seston and sediment has often been observed in shallow estuaries. In eutrophic estuaries in temperate areas, this coupling seems to be explained by the contribution of SPM characteristics to SOM, independent of specific physical characteristics, because phytoplankton production is stimulated in nutrient-rich water column (Carmichael and Valiela, 2005). However, in our oligotrophic tropical estuary, macrophytes, including mangrove-derived debris, contributed significantly to the spatial variation of SOM characteristics, and the vulnerability of the substrate to physical disturbances differed primarily according to the openness of the location to the river and ocean. Therefore, different combinations of various physical factors (i.e., episodic wind and periodic tidal current-induced disturbance, river water inputs, and water depth) caused resuspension at different spatiotemporal timings, resulting in a variety of SPM characteristics in shallow subtidal areas. The postulated sources and transportation of SPM through sediment resuspension were successfully derived by separately estimating the values of background and additional SPM levels for each event. Clarification of the mechanisms of SPM increase, such as by natural disturbance leading to resuspension, can facilitate future research to discriminate the impacts of increasing anthropogenic inputs on SPM dynamics, especially in regard to the tremendous inputs of riverine POM during the rainy season.

Acknowledgements

This study was supported by JSPS (Japan Society for the Promotion of Science) Research Fellowships for Young Scientists (No.10639), CREST (Core Research for Evolutional Science and Technology) managed by JST (Japan Science and Technology) and the Grant-in-Aid for international scientific research program “Conservation of Tropical Seagrass Beds with Special Reference to their Role on Function of Coastal Ecosystem” (No.09041147) from the Ministry of Education, Culture, Sports, Science and Technology, Japan. We thank the staff and students of Ranong Coastal Resources Research

Station of Kasetsart Univ, Thailand for their supports of our field research. M. Minagawa and T. Kuramoto (Hokkaido Univ.) and I. Narushima (AIST) helped us to analyze chemical components in POM and sediments. T. Miyajima, K. Suetsugu, Y. Tanaka (The Univ. of Tokyo) and H. Yamano (National Institute of Environmental Studies) engaged us in stimulating discussions about the data. Z. Forsman and K. McClanahan (Univ. of Hawaii) and S. Rosenblatt helped edit this manuscript.

Literature Cited

Andrews, J.E., Greenaway, A.M., Dennis, P.F. 1998. Combined carbon isotope and C/N ratios as indicators of source and fate of organic matter in a poorly flushed, tropical estuary: Hunts Bay, Kingston Harbour, Jamaica. Estuarine, Coastal and Shelf Science 46, 743-756.

Alvarez, L.G., Jones, S.E., 2002. Factors influencing suspended sediment flux in the upper Gulf of California. Estuarine, Coastal and Shelf Science 54, 747-759.

Bacon, G.S., MacDonald, B.A., Ward, J.E., 1998. Physiological responses of infaunal (*Mya arenaria*) and epifaunal (*Placopecten magellanicus*) bivalves to variations in the concentration and quality of suspended particles: I. Feeding activity and selection. Journal of Experimental Marine Biology and Ecology 219, 105-125.

Benner, R., Hatcher, P.G., Hedges, J.I., 1990. Early diagenesis of mangrove leaves in a tropical estuary: Bulk chemical characterization using solid-state ^{13}C NMR and elemental analyses. Geochimica et Cosmochimica Acta 54, 2003-2013.

Blanchard, G.F., Guarini, J.M., Orvain, F., Sauriau, P.G., 2001. Dynamic behavior of benthic microalgal biomass in intertidal mudflats. Journal of Experimental Marine Biology and Ecology 264, 85-100.

Bodineau B., Thoumelin G., Béghin V., Wartel M., 1998. Tidal time-scale changes in the composition of particulate organic matter within the estuarine turbidity maximum zone in the macrotidal Seine Estuary, France: the use of fatty acid and sterol biomarkers. Estuarine, Coastal and Shelf Science 47, 37-49.

Carmichael R.H., Valiela I., 2005. Coupling of near-bottom seston and surface sediment composition: Changes with nutrient enrichment and implications for estuarine food supply and biogeochemical processing. Limnology and Oceanography 50, 97-105.

Cifuentes, L.A., Sharp, J.H., Fogel, M.L., 1988. Stable carbon and nitrogen isotope biogeochemistry in the Delaware estuary. Limnology and Oceanography 33, 1102-1115.

Cifuentes, L.A., Coffin, R.B., Solorzano, L., Cardenas, W., Espinoza, J., Twilley R.R., 1996. Isotopic and elemental variations of carbon and nitrogen in a mangrove estuary. Estuarine, Coastal and Shelf Science 43, 781-800.

Correll D.L., Jordan T.E., Weller, D.E., 2001. Effects of precipitation, air temperature, and land use on organic carbon discharges from Rhode River watersheds. Water Air and Soil Pollution 128, 139-159.

Dittmar, T., Lara, R.J., Kattner, G., 2001. River of mangrove? Tracing major organic matter sources in

tropical Brazilian coastal waters. Marine Chemistry 73, 253-271.

Douglas, R.W., Rippey, B., 2000. The random redistribution of sediment by wind in a lake. Limnology and Oceanography 45, 686-694.

Dyer, K.R., Christie, M.C., Feates, N., Fennessy, M.J., Pejrup M., van der Lee W., 2000. An Investigation into processes influencing the morphodynamics of an intertidal mudflat, the Dollard Estuary, The Netherlands: I. Hydrodynamics and suspended sediment. Estuarine, Coastal and Shelf Science 50, 607-625.

Ellis, J., Cummings, V., Hewitt, J., Thrush, S., Norkko, A., 2002. Determining effects of suspended sediment on condition of a suspension feeding bivalve (*Atrina zelandica*): results of a survey, a laboratory experiment and a field transplant experiment. Journal of Experimental Marine Biology and Ecology 267, 147-174.

Furukawa, K., Wolanski, E., Mueller, H., 1997. Currents and sediment transport in mangrove forests. Estuarine, Coastal and Shelf Science 44, 301-310.

Gacia, E., Duarte, M.D., Middelburg, J.J., 2002. Carbon and nutrient deposition in a Mediterranean seagrass (*Posidonia oceanica*). Limnology and Oceanography 47, 23-32.

Gibbs, R.J., Konwar, L., 1986. Coagulation and settling of Amazon River suspended sediment. Continental Shelf Research 6, 127-149.

Goñi, M.A., Teixeira, M.J. Perkey, D.W., 2003. Sources and distribution of organic matter in a river-dominated estuary (Winyah Bay, SC, USA). Estuarine, Coastal and Shelf Science 57, 1023-1048.

Hemminga, M.A., Slim, F.J., Kazungu, J., Ganssen, G.M., Nieuwenhuize, J., Kruyt, N.M., 1994. Carbon outwelling from a mangrove forest with adjacent seagrass beds and coral reefs (Gazi Bay, Kenya). Marine Ecology Progress Series 106, 291-301.

Howarth, R.W., Fruci, J.R. Sherman, D., 1991. Inputs of sediment and carbon to an estuarine ecosystem: Influence of land-use. Ecological Application 1, 27-39.

Ishihara, K., 1990. Statistics for Bioscience. Nankodo, Tokyo, p.378.

Jackson, C., Preston, N., Thompson, P.J., Burford, M., 2003. Nitrogen budget and effluent nitrogen components at an intensive shrimp farm. Aquaculture 218, 397-411.

Kennedy, H., Gacia E., Kennedy D.P., Papadimitriou S. Duarte C.M., 2004. Organic carbon sources to SE Asian coastal sediments. Estuarine, Coastal and Shelf Science 60, 59-68.

Kuramoto, T., Minagawa, M., 2001. Stable carbon and nitrogen isotopic characterization of organic matter in a mangrove ecosystem on the southwestern coast of Thailand. Journal of Oceanography 57, 421-431.

Longstaff, B.J., Dennison, W.C., 1999. Seagrass survival during pulsed turbidity events: the effects of light deprivation on the seagrasses *Halodule pinifolia* and *Halophila ovalis*. Aquatic Botany 65, 105-121.

Luettich, R.A., Harleman, D.R.F., Somlyody, L., 1990. Dynamic behavior of suspended sediment concentrations in a shallow lake perturbed by episodic wind events. Limnology and Oceanography 35, 1050-1067.

Madsen, J.D., Chambers, P.A., James, W. F., Koch, E.W., Westlake, D.F., 2001. The interaction between water movement, sediment dynamics and submersed macrophytes. Hydrobiologia 444, 59-68.

Mazda, Y., Sato, Y., Sawamoto, S., Yokochi, H., Wolanski, E., 1990. Links between physical, chemical and biological process in Bashita-minato, a mangrove swamp in Japan. Estuarine, Coastal and Shelf Science 31, 817-833.

Meksumpun, S., Meksumpun, C., 2002. Stable carbon and nitrogen isotope ratio of sediment in Ban Don Bay: Evidence for understanding sources of organic matters in the coastal environment. Kasetsart Journal (Natural Science) 36, 75-82.

Midwood, A., Boutton, T.W., 1998. Soil carbonate decomposition by acid has little effect on $\delta^{13}C$ of organic matter. Soil Biology and Biochemistry 30: 1301-1307.

Miyajima, T., Koike, I., Yamano, H., Iizumi, H., 1998. Accumulation and transport of seagrass-derived organic matter in reef flat sediment of Green Island, Great Barrier Reef. Marine Ecology Progress Series 175, 251-259.

Moore K.A., Wetzel, R.L., 2000. Seasonal variations in eelgrass (*Zostera marina L.*) responses to nutrient enrichment and reduced light availability in experimental ecosystems. Journal of Experimental Marine Biology and Ecology 244, 1-28.

Oldham, C.E., Lavery, P.S. 1999 Porewater nutrient fluxes in a shallow fetch-limited estuary. Marine Ecology Progress Series 183, 39-47.

Peterson, C.H., Luettich, R.A. Jr., Micheli, F., Skilleter, G.A., 2004. Attenuation of water flow inside seagrass canopies of differing structure. Marine Ecology Progress Series 268, 81-92.

Preen, A.R., Long, W.J.L., Coles, R.G., 1995. Flood and cyclone related loss, and partial recovery, of more than 1000 km^2 of seagrass in Hervey Bay, Queensland, Australia. Aquatic Botany 52, 3-17.

Rezende, C.E., Lacerda L.D., Ovalle, A.R.C., Silva, C.A.R., Martinelli, L.A., 1990. Nature of POC transport in a mangrove ecosystem: A carbon stable isotopic study. Estuarine, Coastal and Shelf Science 30, 641-645.

Sanford, L.P., 1994. Wave-forced resuspension of upper Chesapeake Bay muds. Estuaries, 17(1B), 148-165.

Schubert, C.J., Nielsen, B., 2000. Effects of decarbonation treatments on $\delta^{13}C$ values in marine sediments. Marine Chemistry 72, 55-59.

Schweizer, M., Fear, J., Cadisch, G., 1999. Isotopic (^{13}C) fractionation during plant residue decomposition and its implications for soil organic matter studies. Rapid Communication in Mass Spectrometry 13, 1284-1290.

Smaal, A.C., Haas, H.A., 1997. Seston dynamics and food availability on mussel and cockle beds. Estuarine, Coastal and Shelf Science 45, 247-259.

Suzuki, R., Ishimaru, T., 1990. An improved method for the determination of phytoplankton chlorophyll using by N, N-dimethylformamide. Journal of Oceanography 46, 190-194.

Suzuki, T., 2003. Distributions and population densities of *Enhalus acoroides* and *Anadara* sp. attached to *Enhalus* bodies in the seagrass beds of Andaman Sea, Ranong, Thailand, pp. 135-148. In: I. Koike (eds.), Conservation of tropical seagrass beds with special reference to their role on function of coastal ecosystem.

Tanaka Y., Nakaoka M., 2006. Morphological variation in the tropical seagrasses, *Cymodocea serrulata* and *C. rotundata*, in response to sediment conditions and light attenuation. Botanica Marina 49, 365-371.

Trott, L.A., Alongi, D.M., 2000. The impact of shrimp pond effluent on water quality and phytoplankton biomass in a tropical mangrove estuary. Marine Pollution Bulletin 40, 947-951

Tylor, J.R., 1997. An introduction to error analysis-the study of uncertainties in physical measurement. University Science Books, Sausalito. p.327

Uchiyama, Y., 2001. Sediment suspension and short-term morphological response in winter on Banzu intertidal sand-flat, Tokyo Bay, Japan. Journals of the Japan Society of Civil Engineers, No. 677/II-55, 129-140. (in Japanese, with English Abstr).

Umezawa, Y., Miyajima, T., Koike, I. (2008) Stable nitrogen isotope composition in sedimentary organic matter as a potential proxy of nitrogen sources for primary producers at a fringing coral reef. Journal of Oceanography, 64, 899-909

Widdows, J, Brown, S., Brinsley, M. D., Salkeld, P.N., Elliott, M., 2000. Temporal changes in intertidal sediment erodability: influence of biological and climatic factors. Continental Shelf Research 20, 1275-1289.

Wolanski, E., 1995. Transport of sediment in mangrove swamps. Hydrobiologia 295, 31-42.

Wolanski, E., Spagnol, S., 2003. Dynamics of the turbidity maximum in King Sound, tropical Western Australia. Estuarine, Coastal and Shelf Science 56, 877-890.

Yamamuro, M., Kayanne, H., 1995. Rapid direct determination of organic carbon and nitrogen in

carbonate-bearing sediments with a Yanaco MT-5 CHN analyzer. Limnology and Oceanography 40, 1001-1005.

Yamamuro, M., Umezawa, Y., Koike, I., 2004. Internal variations in nutrient concentrations and C and N stable isotope ratios in the leaves of the seagrass *Enhalus acoroides*. Aquatic Botany 79, 95-102.

Zimmerman, A.R., and Canuel, E.A., 2001. Bulk organic matter and lipid biomarker composition of Chesapeake Bay surficial sediments as indicators of environmental processes. Estuarine, Coastal and Shelf Science 53, 319-341.

Figure Captions

Figure 1: Location of the study area. The three open circles indicate the sampling and monitoring stations at each subtidal seagrass bed. The 33 sediment sampling stations are indicated in the box in the upper right.

Figure 2: Turbidimeter calibration derived from *in situ* a) POC and b) SPM data collected hourly at each monitoring site. The values in near-bottom water were plotted in logarithmic scales. Turbidimeter output was calibrated in the laboratory to fine clay, kaolin-based values (mg L^{-1}). One outlier at MH was omitted from the calculations.

Figure 3: Distribution of a) C/N molar ratio, b) $\delta^{13}C$ values, and c) TOC contents for the upper (0-10 mm) layer of coastal sediments. Contour lines represent an interval of 2.0 for the C/N ratio, 1.0‰ for $\delta^{13}C$, and 0.1% for TOC contents.

Figure 4: Relationships between the C/N molar ratio and $\delta^{13}C$ (‰) in sediment. Numbers (1 to 33) refer to the sampling points shown in Figure 1. Ovals indicate the categorization of the sedimentary organic matter. The off-scale values of mangrove leaves (Kuramoto and Minagawa, 2001), epiphytes (Y. Umezawa, unpublished data), seagrasses (*Enhalus acoroides*, Yamamuro et al., 2004) and POM in the Khula River (M. Minagawa, unpublished data) are also plotted with error bars.

Figure 5: Time-series variations in physical and chemical parameters monitored at TND on 9, 11, and 14 December 2001. From the top, SPM and POC converted from turbidimeter output, current speed and direction (north at the top of the page), salinity, wind speed, POC/SPM, POC/chl *a*, POC, POC/N, $\delta^{13}C$ in POC and chl *a* are shown on a daily basis. "n.d." indicates no data. The bar on the upper frame indicates high tide and that on the lower frame indicates slack tide. POC samples marked with "*" were considered to be representative values under steady conditions, and used as background values in later calculations (Appendix 1). Similarly, the POC samples bearing large POC loads indicated with "e" were used to estimate the source of additional SPM (Appendix 1). Each datum and error bar represents the mean values of two replicates and their difference. In most cases, the error bars are smaller than the symbols. The events indicated with I, II, III, IV, and V in circles are explained in the text.

Figure 6: Time-series variations in physical and chemical parameters monitored at MH on 22, 23,

and 27 December 2002. The variation of each parameter and other symbols are described in the same manner as those in Fig. 5.

Figure 7: Time-series variations in physical and chemical parameters monitored at KC on 25 and 26 December 2002. The variation of each parameter and other symbols are described in the same manner as those in Fig. 5.

Figure 8: Estimated C/N ratio and $\delta^{13}C$ values in additional SPM compared to background values. Additional SPM values estimated at TND, MH, and KC are characterized in the diagram of sedimentary organic matter characteristics (Fig. 4) with red upward-pointing triangles, yellow circles, and blue squares, respectively. Larger symbols with dots in the center are the values of POM under steady conditions. The plots of estimated SPM values are categorized for each area and for tidal conditions by oval enclosures.

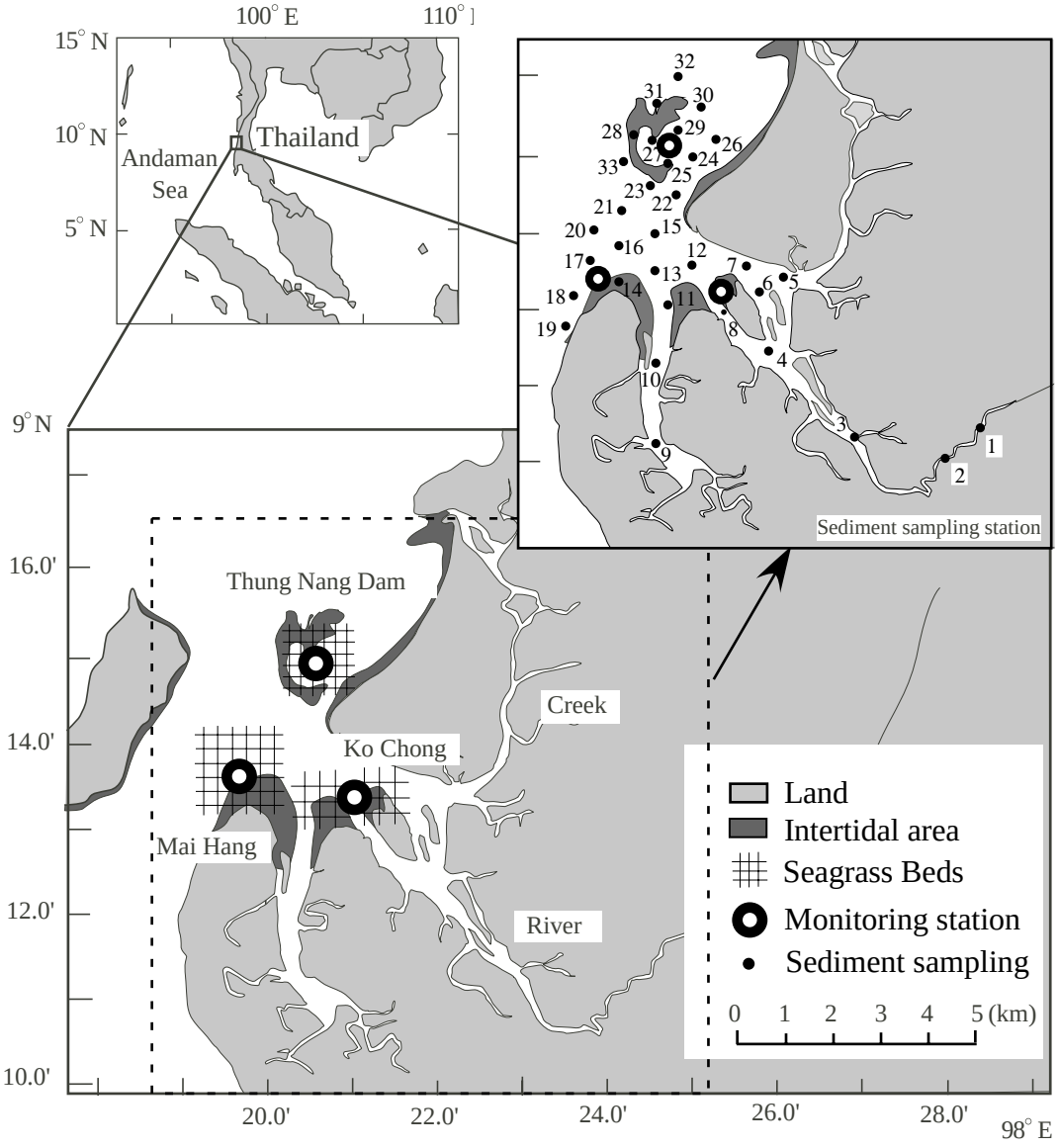

Figure 1: Location of the study area.
The three open circles indicate the sampling and monitoring stations at each subtidal seagrass bed. The 33 sediment sampling stations are indicated in the box in the upper right.

Umezawa et al. Fig. 1

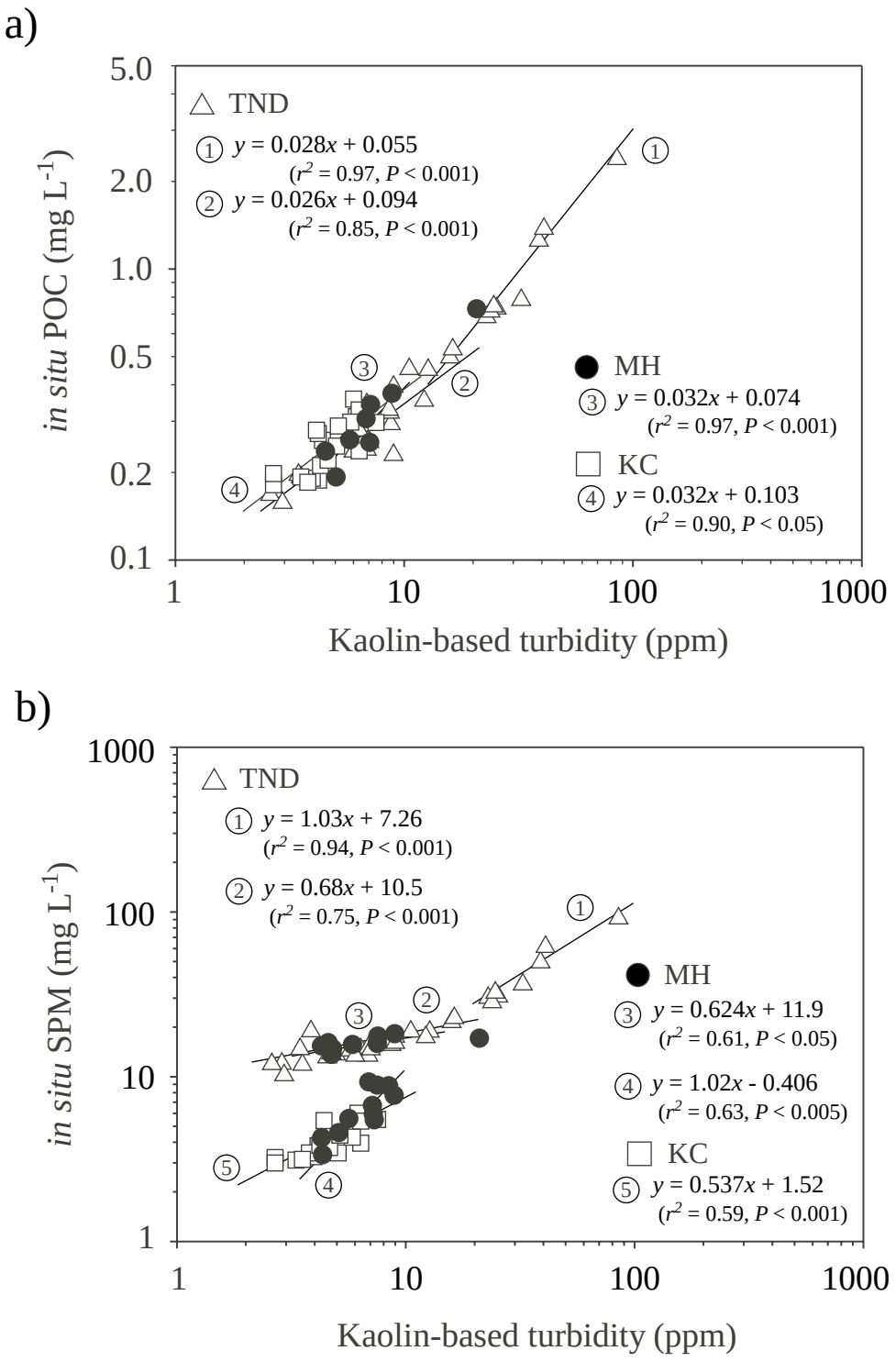

Figure 2: Turbidimeter calibration derived from in situ a) POC and b) SPM data collected hourly at each monitoring site.
The values in near-bottom water were plotted in logarithmic scales. Turbidimeter output was calibrated in the laboratory to fine clay, kaolin-based values (mg L^{-1}). One outlier at MH was omitted from the calculations.

Umezawa et al. Fig. 2

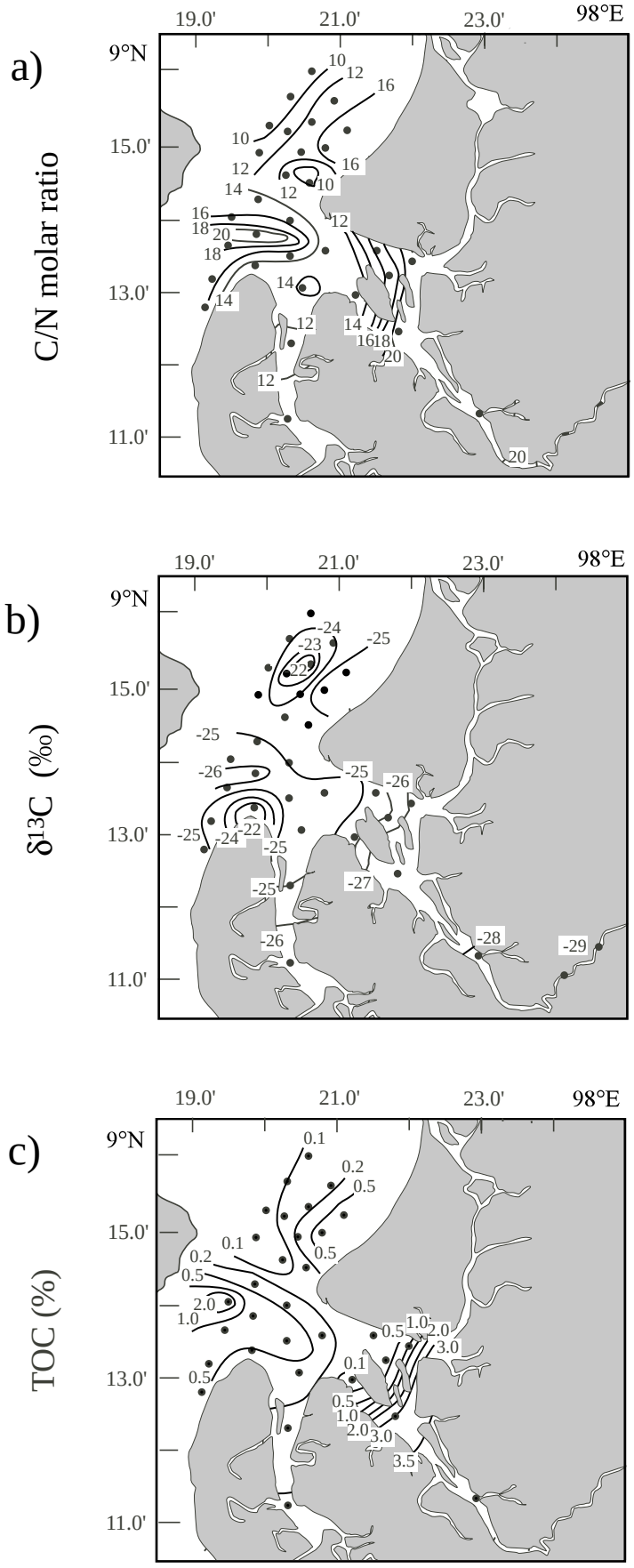

Figure 3: Distribution of a) C/N molar ratio, b) $\delta^{13}C$ values, and c) TOC contents for the upper (0-10 mm) layer of coastal sediments.
Contour lines represent an interval of 2.0 for the C/N ratio, 1.0‰ for $\delta^{13}C$, and 0.1% for TOC contents.

Umezawa et al. Fig. 3

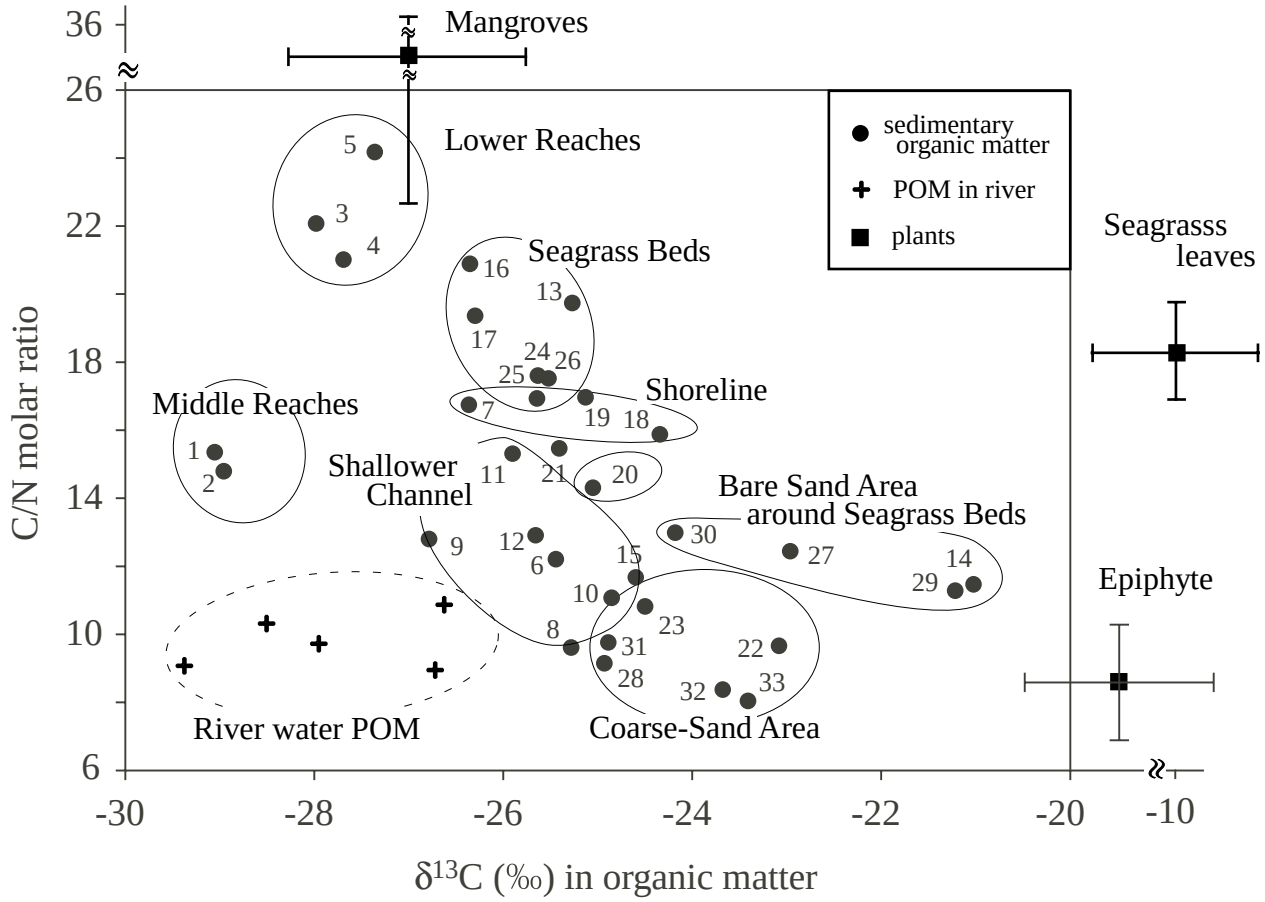

Figure 4: Relationships between the C/N molar ratio and $\delta^{13}C$ (‰) in sediment.

Numbers (1 to 33) refer to the sampling points shown in Figure 1. Ovals indicate the categorization of the sedimentary organic matter. The off-scale values of mangrove leaves (Kuramoto and Minagawa, 2001), epiphytes (Y. Umezawa, unpublished data), seagrasses (*Enhalus acoroides*, Yamamuro et al., 2004) and POM in the Khula River (M. Minagawa, unpublished data) are also plotted with error bars.

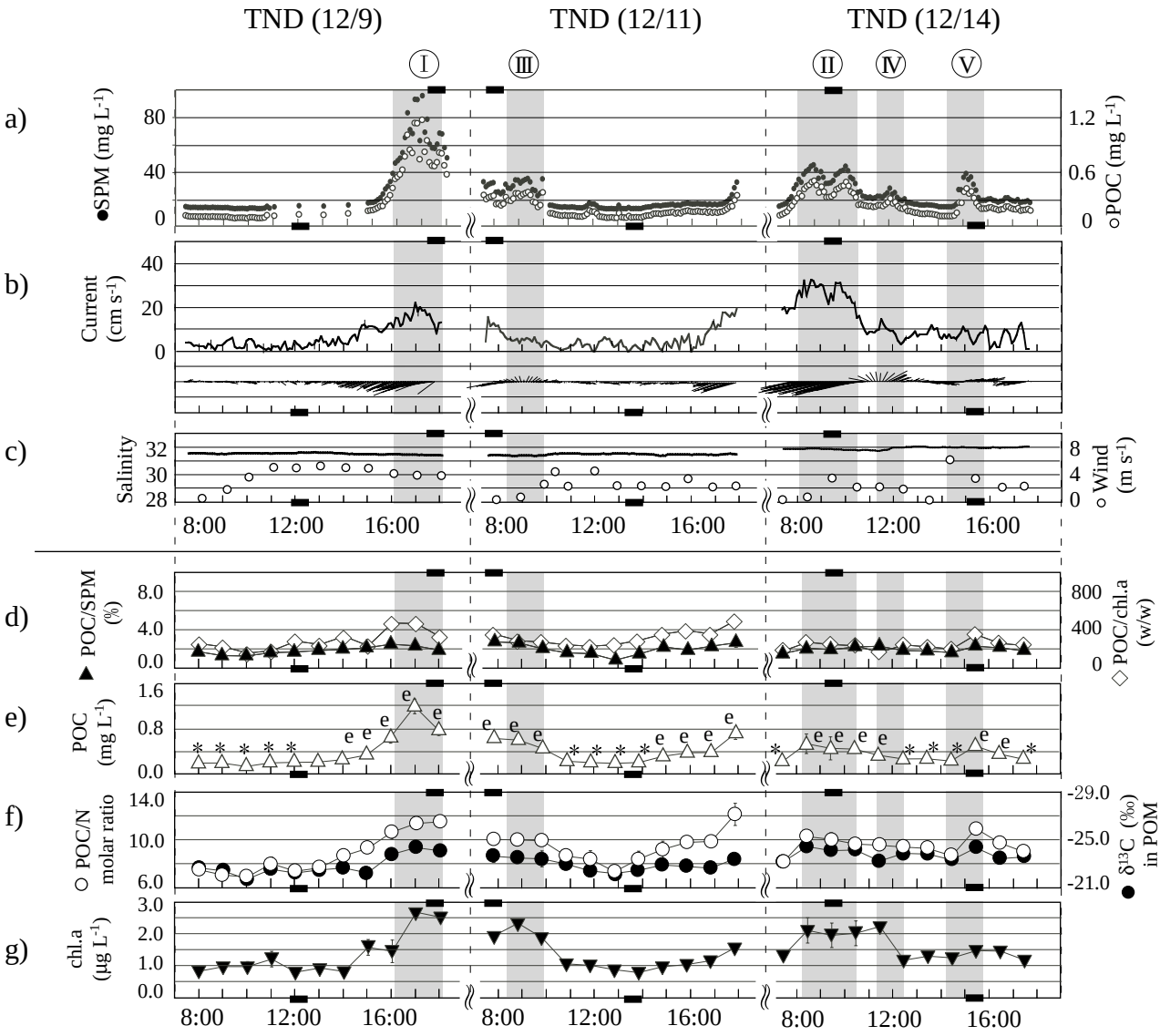

Figure 5: Time-series variations in physical and chemical parameters monitored at TND on 9, 11, and 14 December 2001.

From the top, SPM and POC converted from turbidimeter output, current speed and direction (north at the top of the page), salinity, wind speed, POC/SPM, POC/chl *a*, POC, POC/N, $\delta^{13}C$ in POC and chl *a* are shown on a daily basis. "n.d." indicates no data. The bar on the upper frame indicates high tide and that on the lower frame indicates slack tide. POC samples marked with "*" were considered to be representative values under steady conditions, and used as background values in later calculations (Appendix 1). Similarly, the POC samples bearing large POC loads indicated with "e" were used to estimate the source of additional SPM (Appendix 1). Each datum and error bar represents the mean values of two replicates and their difference. In most cases, the error bars are smaller than the symbols. The events indicated with I, II, III, IV, and V in circles are explained in the text.

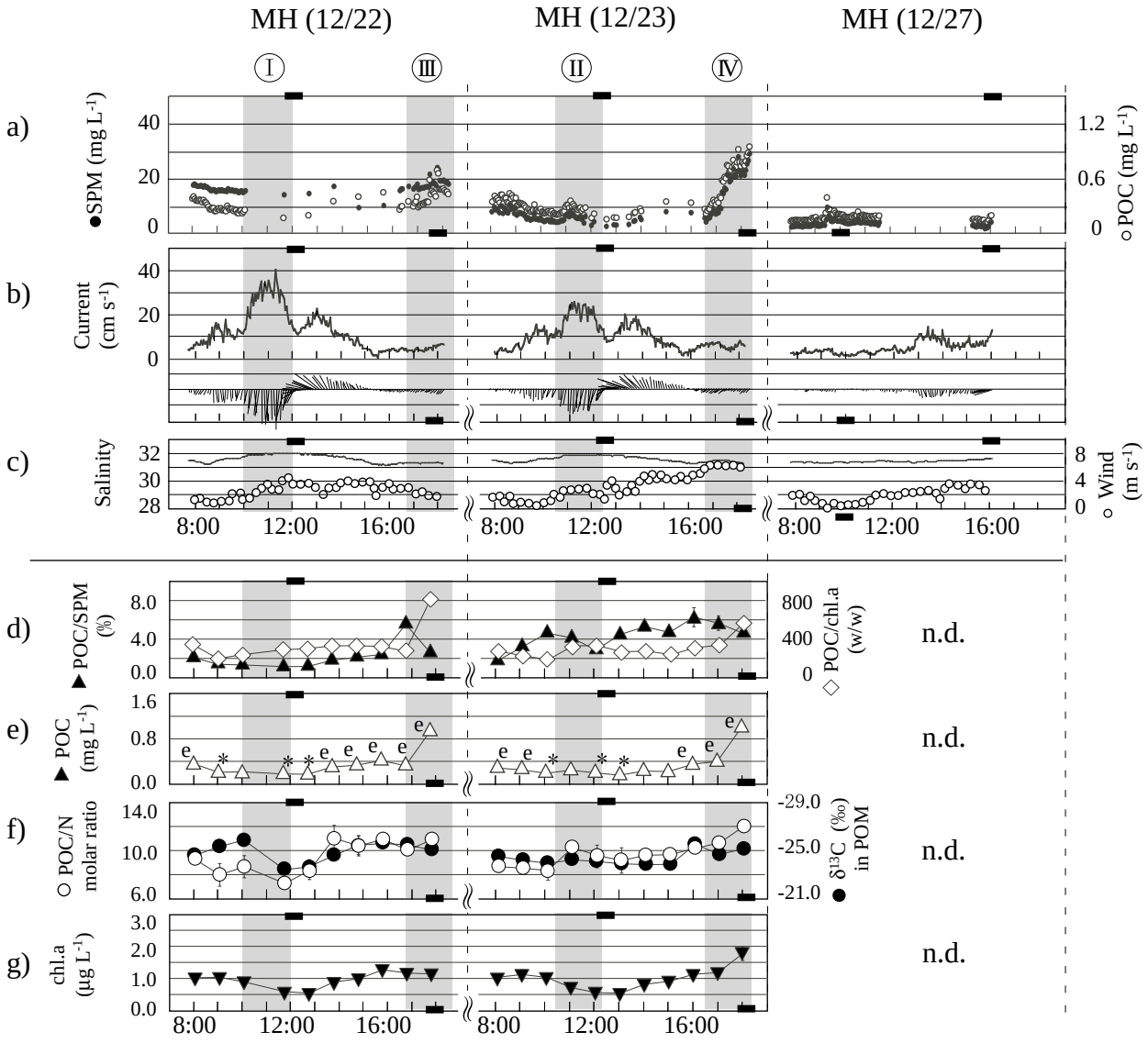

Figure 6: Time-series variations in physical and chemical parameters monitored at MH on 22, 23, and 27 December 2002.
The variation of each parameter and other symbols are described in the same manner as those in Fig. 5.

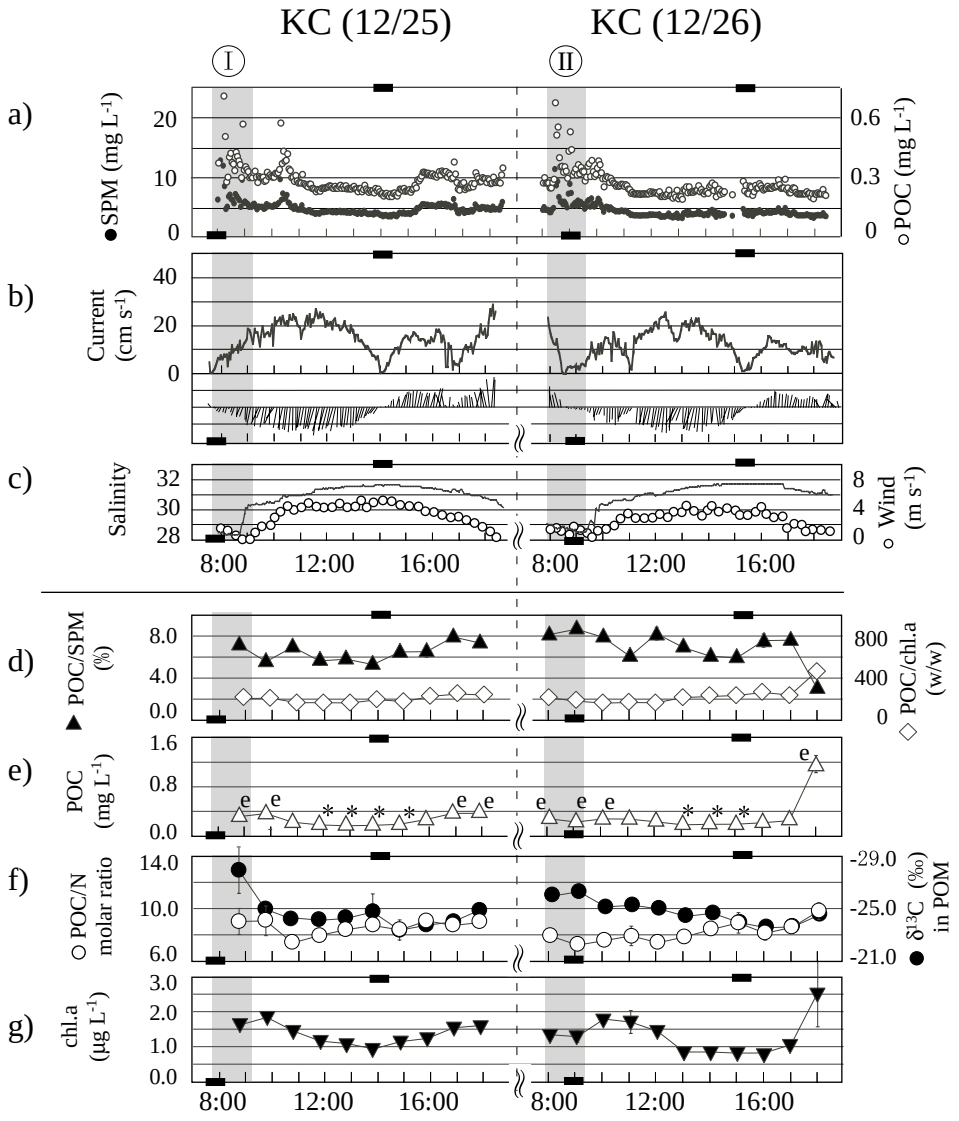

Figure 7: Time-series variations in physical and chemical parameters monitored at KC on 25 and 26 December 2002.
The variation of each parameter and other symbols are described in the same manner as those in Fig. 5.

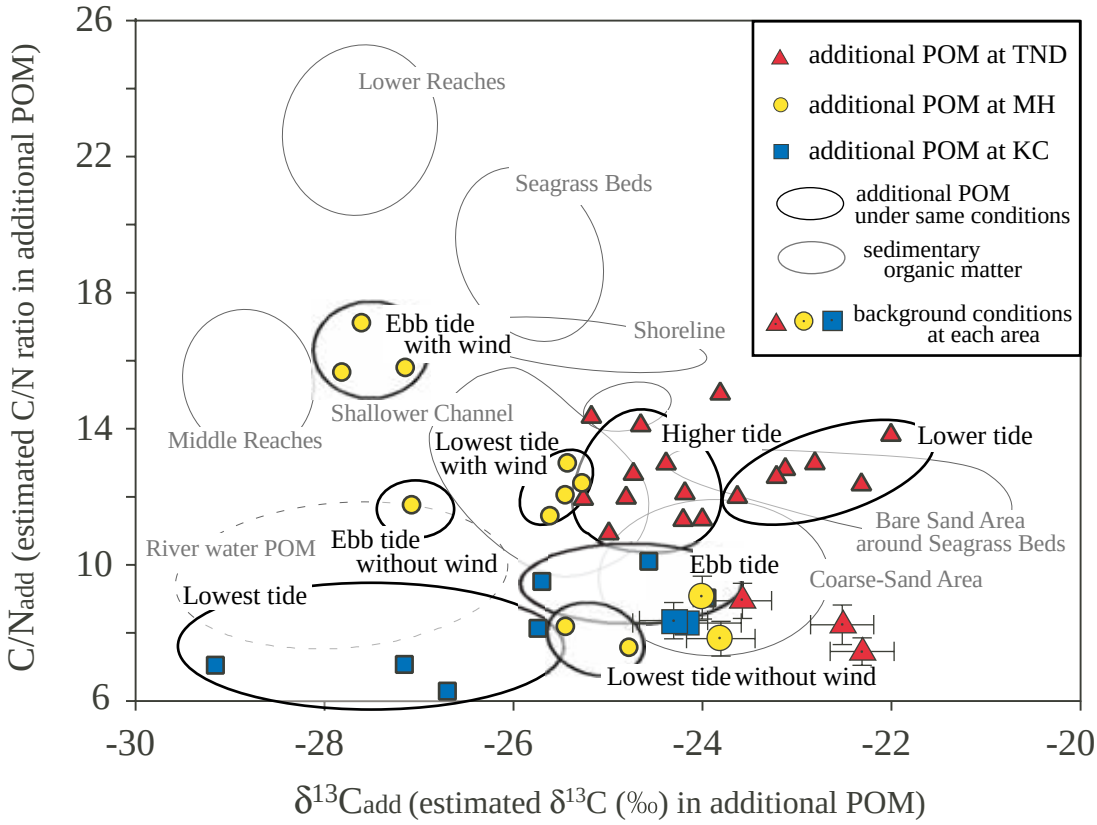

Figure 8: Estimated C/N ratio and $\delta^{13}C$ values in additional SPM compared to background values.

Additional SPM values estimated at TND, MH, and KC are characterized in the diagram of sedimentary organic matter characteristics (Fig. 4) with red upward-pointing triangles, yellow circles, and blue squares, respectively. Larger symbols with dots in the center are the values of POM under steady conditions. The plots of estimated SPM values are categorized for each area and for tidal conditions by oval enclosures.

Umezawa et al. Fig. 8

Table 1. Spearman's correlation coefficients (r_s) between turbidimeter-calibrated SPM and other environmental factors at each location

Location	n	Water Depth	Factor correlated to SPM increase, r_s and (significance)		
			Current Velocity	Wind Velocity	Salinity
TND	277	**0.54** ($p < 0.001$)	**0.69** ($p < 0.001$)	**0.25** ($p < 0.001$)	**-0.13** ($p < 0.05$)
MH	294	**-0.28** ($p < 0.001$)	0.07 ($p < 0.001$)	**0.35** ($p < 0.001$)	**-0.14** ($p < 0.05$)
KC	407	**-0.56** ($p < 0.001$)	-0.14[b] ($p = 0.005$)	-0.36[b] ($p < 0.001$)	**-0.58** ($p < 0.001$)

[a] The values in bold indicate physical factors potentially contributing to an increase in SPM.

[b] Because negative correlations between turbidity and current or wind velocity can be ascribed to multicollinearity among physical factors, the contribution of the applied physical factor to turbidity increase was considered to be minor at each location.

[c] Among the parameters showing simple correlation with SPM increase, no multicollinearity was observed in the data at TND ($r_s = 0.10$, $p = 0.086$ for current vs. wind; $r_s = 0.05$, $p = 0.447$ for current vs. salinity; and $r_s = -0.11$, $p = 0.069$ for wind vs. salinity; Spearman's rank correlation), while a weak correlation was observed at MH ($r_s = 0.31$, $p < 0.001$ for wind vs. salinity).

Table 2. Results of multiple regression analysis: the significance of each physical factor causing an increase of SPM at TND and MH.

Location	Adjusted r^2	ANOVA	Standardized partial regression coefficients and their significance		
		F -value of *F* -test	Current Speed[a]	Wind Speed[a]	Salinity[a]
TND	0.42	**67.3** > $\boldsymbol{F}_{(3, 276)}(0.05) = 2.6$	**0.63** ($p < 0.001$)	**0.26** ($p < 0.001$)	-0.06 ($p = 0.338$)
MH	0.30	**49.2** > $F_{(2, 293)}(0.05) = 3.0$	—	**0.50** ($p < 0.001$)	**-0.18** ($p < 0.001$)

[a] The factors selected as independent variables were those estimated by simple regression analysis to have potentially contributed to an increase in turbidity.

[b] Dependent variables (SPM mg/L) at TND and MH were log transformed [*log* (SPM-a); a=2.0 for TND, a=1.5 for MH] to render their distributions normal (Ichihara, 1990).

Appendix 1. Estimated C/N ratios and $\delta^{13}C$ values of additional POC under high turbidity conditions.

Site	date	time	tide[b]	Background POC			Observed POC			Estimated POC			
				POC_{bg} mg L^{-1}	PON_{bg} mg L^{-1}	$\delta^{13}C_{bg}$ (‰)	POC_{ob} mg L^{-1}	PON_{ob} mg L^{-1}	$\delta^{13}C_{ob}$ (‰)	C/N_{add}[a] molar ratio	SD	$\delta^{13}C_{add}$ (‰)	SD[c]
TND	9 Dec.	15:00	L				0.3	0.04	-22.2	**13.8**	5.4	**-22.0**	6.2
		16:00	H	0.19	0.030	-22.4	0.7	0.07	-23.8	**12.9**	1.5	**-24.4**	2.1
		17:00	H	(8:00 - 13:00)			1.2	0.12	-24.3	**12.6**	0.7	**-24.7**	1.0
		18:00	H				0.8	0.08	-24.1	**14.1**	4.3	**-24.6**	8.5
	11 Dec.	8:00	H				0.6	0.07	-23.6	**11.3**	1.4	**-24.2**	4.3
		9:00	H				0.6	0.07	-23.5	**11.3**	1.9	**-24.0**	5.3
		10:00	H	0.20	0.028	-22.5	0.4	0.05	-23.4	**12.0**	3.3	**-24.2**	9.1
		15:00	L	(11:00 - 14:00)			0.3	0.04	-22.9	**11.9**	4.4	**-23.6**	11.2
		16:00	L				0.4	0.04	-22.8	**12.7**	3.0	**-23.1**	7.4
		17:00	L				0.4	0.04	-22.6	**12.9**	2.7	**-22.8**	6.6
		18:00	H				0.7	0.06	-23.4	**15.0**	3.4	**-23.8**	7.2
	14 Dec.	9:00	H				0.5	0.06	-24.5	**11.9**	1.9	**-25.2**	3.4
		10:00	H				0.5	0.05	-24.1	**11.9**	2.8	**-24.8**	5.1
		11:00	H	0.26	0.033	-23.7	0.4	0.05	-24.2	**10.9**	2.6	**-25.0**	5.7
		12:00	L	(8:00, 13:00 - 15:00, 18:00)			0.3	0.04	-23.3	**12.3**	6.9	**-22.3**	13.1
		16:00	L				0.5	0.05	-24.4	**14.3**	3.1	**-25.2**	4.0
		17:00	L				0.4	0.04	-23.5	**12.5**	8.0	**-23.2**	14.1
MH	22 Dec.	8:00	L				0.4	0.04	-24.7	**11.3**	2.7	**-25.6**	4.7
		13:40	E				0.3	0.03	-24.7	**30.1**	24.6	**-26.0**	8.2
		14:40	E	0.21	0.027	-23.8	0.3	0.04	-25.5	**17.0**	6.3	**-27.6**	11.7
		15:40	E	(9:00, 11:40 - 12:40)			0.4	0.04	-25.7	**15.7**	3.6	**-27.1**	3.4
		16:40	E				0.3	0.04	-25.5	**15.6**	6.0	**-27.8**	6.2
		17:40	L				0.9	0.10	-25.1	**12.0**	0.7	**-25.4**	1.1
	23 Dec.	8:00	L				0.3	0.04	-24.5	**8.1**	3.6	**-25.4**	12.3
		9:00	L	0.17	0.022	-24.0	0.2	0.03	-24.2	**7.5**	4.3	**-24.7**	15.2
		16:00	E	(10:00, 12:00 - 13:00)			0.3	0.04	-25.5	**11.7**	5.6	**-27.0**	12.0
		17:00	L				0.4	0.04	-24.7	**12.3**	5.5	**-25.2**	8.5
		18:00	L				1.0	0.10	-25.2	**12.9**	1.7	**-25.4**	2.5
KC	25 Dec.	9:00	L				0.3	0.04	-28.0	**9.9**	3.1	**-32.9**	3.5
		10:00	L	0.19	0.026	-24.2	0.4	0.05	-25.0	**8.1**	3.5	**-25.7**	5.5
		17:00	E	(11:00 - 14:00)			0.4	0.05	-24.0	**9.0**	1.1	**-23.9**	2.8
		18:00	L				0.4	0.05	-24.9	**9.5**	1.1	**-25.7**	2.2
	26 Dec.	8:00	L				0.3	0.04	-25.9	**7.0**	2.3	**-29.1**	7.2
		10:00	L	0.18	0.026	-24.1	0.3	0.04	-25.1	**6.2**	0.8	**-26.7**	4.4
		11:00	L	(13:00 - 15:00)			0.3	0.04	-25.2	**7.0**	1.8	**-27.1**	2.2
		18:00	E				1.2	0.14	-24.5	**10.0**	1.6	**-24.5**	4.9

[a] CN_{add} is the molar ratio of C to N.

[b] Samples collected during high, low, and ebb tide conditions are indicated by H, L, and E, respectively.

[c] Standard deviations (SDs) of CN_{add} and $\delta^{13}C_{add}$ were calculated based on the method of Tylor (1997),

When W is explained as $W = aX + bY + cZ + \ldots\ldots$, its standard deviation σ_w is $(a^2\sigma_x^2 + b^2\sigma_v^2 + c^2\sigma_z^2 + \ldots\ldots)^{1/2}$

When W is explained as $W = X^sY^tZ^r \ldots\ldots$, its standard deviation σ_w is $|W| \times ([\sigma_x / X]^2 + [\sigma_v / Y]^2 + [\sigma_z / Z]^2 + \ldots\ldots)^{1/2}$

Because these polynomial equations included many members with errors and resulted in conservative values;

some calculated CN_{add} and $\delta^{13}C_{add}$ values had large errors (i.e., 3.8 for the C/N ratio and 6.4‰ for $\delta^{13}C$ on average).